Journal of Bioscience and Bioengineering
VOL. 127 No. 6, 703–709, 2019

www.elsevier.com/locate/jbiosc

In vitro and *in vivo* inhibition of Hass avocado polyphenol oxidase enzymatic browning by paeonol, β-cyclodextrin, and paeonol:β-cyclodextrin inclusion complex

Anahí Fuentes Campo,[1] Matias I. Sancho,[2,*] Gisela Melo,[2] Yamina A. Dávila,[3] and Estela Gasull[2]

Universidad Nacional de San Luis, Facultad de Química, Bioquímica y Farmacia, Chacabuco 917, 5700 San Luis, Argentina,[1] Universidad Nacional de San Luis, Facultad de Química, Bioquímica y Farmacia, IMIBIO-CONICET, Chacabuco 917, 5700 San Luis, Argentina,[2] and Universidad Nacional de San Luis, Facultad de Química, Bioquímica y Farmacia, INTEQUI-CONICET, Chacabuco 917, 5700 San Luis, Argentina[3]

Received 6 September 2018; accepted 15 November 2018
Available online 17 December 2018

Polyphenol oxidase (PPO) was extracted from Hass avocados and its physicochemical properties were analyzed. The optimum pH and temperature of the enzyme were pH 7.5 and 20°C. This PPO showed a high thermal stability, since 26% of the initial activity was retained by the enzyme after heating at 60°C for 40 min. Inhibition studies were performed using different chemical reagents, and the order in the inhibition efficiency was paeonol > 4-hydroxybenzaldehyde > β-cyclodextrin (β-CD). The first two inhibitors presented a non-competitive mechanism while the inhibition by β-CD results from a mixed type mechanism. Since the aqueous solubility of paeonol (a natural compound) is very low, the inclusion complex between this drug and β-CD was obtained in solution and solid state. The stoichiometry of the paeonol:β-CD complex was 1:1 and its ΔG° of formation was −26 kJ/mol. The complexation of paeonol by β-CD not only enhances the aqueous solubility and thermal stability of the drug, but also improves the *in vitro* inhibition efficiency against PPO. Colorimetric analysis on avocados pulp (*in vivo*) showed that the inclusion complex does not increase the inhibitory effect of paeonol, remaining practically unchanged. However, the formulation of paeonol:β-CD inclusion complex allows employing this compound as PPO inhibitor in aqueous solutions.

[**Key words:** Polyphenol oxidase; Avocado; Paeonol; β-Cyclodextrin; Inclusion complex; Enzyme inhibition]

The loss of nutritional and organoleptic properties of fruits and vegetables during postharvesting, storing and processing is a main problem in food industry. Several physical and chemical processes are responsible for this issue, but one of the most important is the browning effect (1). The browning mechanism in foods is a well-known phenomenon and it can be of enzymatic or non-enzymatic origin. The enzymatic browning is due to the catalytic activity of a copper-containing family of isoenzymes named polyphenol oxidases (PPO). The PPO catalyzes the oxidation reaction of *o*-diphenols, present in the tissue of fruits and vegetables, with molecular oxygen into *o*-quinones. These *o*-quinones later polymerized with other *o*-quinones and other substances to produce dark brown pigments (2). According to this, the control of enzymatic browning is of great industrial interest and many investigations on this subject are constantly under development (3–5). The activity of PPO can be attenuated by using physical methods such as thermal treatments (blanching) (6), UV radiation (7), ultrasound (8) and pulsed electric fields (9) or by the addition of chemical reagents. There are reports of a wide variety of compounds with PPO inhibitory effect. Naturally occurring organic acids like citric, ascorbic, cinnamic and oxalic acid are frequently employed as PPO inhibitors (10,11). Other natural compounds like flavones and chalcones (12) and inorganic salts like sodium bisulfite are also effective inhibitors of this enzyme. Although PPO is found in many fruits and vegetables, the activity of this enzyme may be different depending on the source. Avocado PPO has a high catalytic activity and a considerable resistance to common inhibition treatments compared with PPOs from other fruits (13,14). For this reason, the inhibition of avocado PPO is not a simple task. For an industrial processing of the fruits the quality of the pulp must be preserved, reducing the PPO activity as low as possible.

Paeonol (2′-hydroxy-4′-methoxy-acetophenone) is a natural compound extracted from the root bark of *Paeonia suffructicosa* Andrews and *Cynanchum paniculatum* (Bunge) Kitagawa (15). Frequently employed in traditional Chinese medicine, paeonol possess multiple pharmacological properties including analgesic, anti-inflammatory, anti-atherosclerosis, anti-tumoral and neuroprotective effects (16,17). Taking into account the similarity between the molecular structure of paeonol and the substrates of PPO (polyphenols) it is reasonable to think that this natural compound could have inhibitory effects of the enzyme catalytic activity. Despite the biological properties of paenol, the aqueous solubility of this compound is very low, limiting it potential use as food additive. To overcome this limitation, the formation of inclusion complexes with cyclodextrins (CDs) is a frequently employed technique designed to increase the aqueous solubility of hydrophobic drugs (18–21). CDs are nontoxic cyclic oligosaccharides of α-D-glucopyranose that can be obtained from the biotransformation of starch. The most common CDs are formed by six (α-CD),

* Corresponding author. Tel.: +54 266 4520300 int. 1655; fax: +54 2652 430224.
E-mail address: misancho@unsl.edu.ar (M.I. Sancho).

1389-1723/$ – see front matter
https://doi.org/10.1016/j.jbiosc.2018.11.009

seven (β-CD), or eight glucose subunits (γ-CD). Taking into account the cavity dimensions, low cost and higher productive rate, β-CD represents the 97% of CDs use in the industry (20). A notable increase in the use of CDs as food additives and in food processing has been observed in recent years. In addition to solubility enhancements, CDs present applications such as the stabilization of fragrances, flavorings and essential oils against unwanted changes; the suppression of unpleasant odors and flavors and the protection of compounds present in multi-component foods against various methods of processing and heat treatment (20–23).

There are few reports in the literature regarding the inhibitory effects of paeonol on PPO, however all these studies employed a commercial PPO extracted from mushrooms (24,25). To the best of our knowledge, there are no reports of the inhibition of PPO by paeonol employing the enzyme extracted from fresh vegetables or fruits. In the present work the physicochemical characterization of PPO from avocado (cv. Hass) was performed and the effect of paeonol on the enzymatic browning was analyzed. Moreover, the inclusion complex of this compound with β-CD was prepared and characterized. The inhibitory effects of paeonol, β-CD and the inclusion complex were evaluated by means of *in vitro* experiments. Finally, the enzymatic browning inhibition of these agents was also analyzed directly on the avocado pulps using a colorimetric method (*in vivo*).

MATERIALS AND METHODS

Reagents Whole fruits of avocado (*Persea americana*, cv. Hass) were purchased at commercial maturity from a local market in San Luis, Argentina and stored at 4°C until used in the experiments. Paeonol (2′-hydroxy-4′-methoxy-acetophenone), catechol, and 4-hydroxybenzaldehyde were purchased from Sigma–Aldrich (St. Louis, MO, USA). Triton X-100 was purchased from Fluka (Buchs, Switzerland). β-CD was obtained from M.P. Biomedicals (Santa Ana, CA, USA) and used without further purification. Spectroscopic grade ethanol was acquired from Merck, and double distilled water was purified using a Thermo Fisher Scientific Easypure II system (Thermo Fisher Scientific, Marietta, OH, USA), with conductivity lower than 1.8 μS cm^{-1}.

PPO extraction and activity assay The extraction of PPO from Hass avocados was performed following a previously reported procedure (26). The flesh of four ripe fruits (100 g) were peeled and homogenized in a commercial blender for 2 min with 100 mL of a buffer solution (pH 6.5). The buffer was prepared with a 50 mM sodium phosphate solution, containing ascorbic acid (20 mM), polyethylenglycol (2% v/v) and Triton X-100 (1% v/v). Polyethylenglycol was used to bind phenols which could inactivate PPO activity during the extraction, and Triton X-100, a non-ionic surfactant, was employed to improve the extraction of the enzyme (27). After filtration of the mixture with gauze, the filtrate was centrifuged at 15,000 rpm for 30 min in a Beckman Coulter J2-HS ultracentrifuge (Beckman Coulter, Fullerton, CA, USA) with the temperature set at 4°C. The supernatants were recovered and kept in tubes at −20°C and used as crude enzyme extract. The enzyme activity assay was carried out by registering the rate of increase in the absorbance at 410 nm with a Varian Cary 50 UV-Vis spectrophotometer (Varian, Mulgrave, Australia) equipped with a peltier temperature controller. Reaction rates were computed from the linear slopes of the absorbance-time curves. The reaction mixtures contained 3 mL of buffer solution and appropriate amounts of enzyme and substrate. One unit of PPO activity (UE) was defined as the amount of enzyme that caused an increase in absorbance of 0.001/min (26). For each experiment, the kinetic data was treated according to the Lineweaver–Burk method (28). Michaelis–Menten constant (K_M) and maximum rate (V_{max}) were determined from the linear regression curves. All assays were performed in triplicate.

Effects of pH and temperature The PPO activity was determined in a pH range of 4.0–9.5. Then, at optimum pH value the activity was measured at different temperatures in a range of 10–45°C. The reaction mixture contained 3 mL of buffers solution with 25 μL of catechol (25 mM) and it was kept for 15 min at constant temperature before the addition of 25 μL of the enzyme extract.

Thermal stability Thermal stability of PPO extracted from avocado was analyzed at optimum pH and several constant temperatures. A buffer solution with 25 μL of the enzyme extract was incubated in a Jeio Tech SI-300R shaker (Daejeon, S. Korea) at 20°C, 30°C, 40°C, 50°C and 60°C for different time lapses (10–40 min). After that, the enzyme solution was immediately cooled in an ice bath. Then, 3 mL of the solution was placed in a quartz cell and kept at 20°C. An aliquot of 50 μL of catechol solution (25 mM) was added to the mixture and the remaining activity of PPO was measured. The residual percentage of PPO activity was calculated taking the kinetics parameters of the unheated enzyme as a reference.

Effect of inhibitors *in vitro* and *in vivo* The effect of inhibitors on the PPO activity was examined by means of *in vitro* and *in vivo* experiments. *In vitro* experiments were carried out in quartz cell containing 3 mL of buffer solution (at optimum pH and temperature), 25 μL of the enzyme extract and different amounts (10–60 μL) of catechol solution 25 mM. Increasing volumes of 4-hydroxybenzaldehyde, paeonol, β-CD and the inclusion complex solutions were added in the reaction mixture to test their inhibitory effect. The browning reaction rates were measured by means of UV-Vis spectroscopy. For the *in vivo* experiments, the peeled avocado pulp was homogenized in a blender for 2 min and immediately collected in four separates petri dishes. Three samples were treated with the addition of 5 mL of 1 mM inhibitor solution (paeonol, β-CD, and the inclusion complex) and the remaining sample was kept without any treatment (reference). The color evolution of the samples was measured with an Agrosta Durocolor colorimeter (Agrosta, Serquex, France) for a time lapse of 4 h. Colorimetric data were transformed from RGB space color to $L^* a^* b^*$ space color using the EasyRGB software. The $L^* a^* b^*$ space is an international standard for color measurements, is device-independent and frequently employed to analyze the color of foods. L^* is the lightness or luminance component, while a^* (from green to red) and b^* (from blue to yellow) are the two chromatic components (29). All the measurements were carried out in triplicate.

Formation of paeonol:β-CD inclusion complex in solution and solid state The apparent formation constants and stoichiometry of paeonol:β-CD inclusion complex in aqueous solutions were determined using phase solubility diagrams. To build these diagrams, excess amounts of paeonol (10 mg) were weighted in volumetric flasks containing 5 mL of aqueous solutions with different β-CD concentrations (0–0.6 mM). The flask were placed in a Jeio Tech SI-300R shaker at constant temperature (from 25.0°C to 45.0°C ± 0.1°C) with a shaking rate of 150 rpm for 48 h until equilibrium was reached. The solutions were then filtered with GVS filters (0.45 μm) and appropriately diluted. The concentration of paeonol was determined from spectroscopic measurements at 276 nm. All the experiments were carried out in triplicate.

The solid state inclusion complex were prepared by the freeze-dried method (FD), following known procedures (18). Equimolar amounts of the reagents were dissolved in 100 mL of a mixed ethanol:water solution (1:1, v/v) with magnetic stirring at room temperature for 24 h protected from light to prevent degradation. The solution was then filtered and placed on stainless steel trays, frozen at −40°C, and freeze-dried using an L-A-B4 Rificor lyophilizer (Rificor, Buenos Aires, Argentina) at 1 bar. A physical mixture (PM) of paeonol and β-CD was also prepared by mixing the reagents in a mortar at room temperature. This PM sample was prepared as a reference for comparison purposes.

Solid state characterization of the inclusion complex Fourier transform infrared spectra of paeonol, β-CD, the FD inclusion complex and the physical mixture were registered on a Shimadzu IR Affinity-1 spectrophotometer (Shimadzu, Kyoto, Japan). The spectra were recorded in the 4000–400 cm^{-1} region, using the KBr pellet technique and with a spectral resolution of 2 cm^{-1}. Powder X-ray diffractions were obtained in a Rigaku ULTIMA IV Type II (Rigaku, Tokyo, Japan) diffractometer using Cu Kα radiation (Ni-filter) and NaCl and quartz as external calibration standards. The diffractograms were recorded in the 2θ angle range of 3–50°, and the process parameters were set at 0.02 2θ scan step size and 2 s scan step time. Differential scanning calorimetry (DSC) curves were obtained with a Shimadzu TA-60WS thermal analysis system using 4 mg of the powder in open aluminum pans, in flowing air at 50 mL min^{-1}, and a heating rate of 10°C min^{-1} from room temperature to 400°C. An empty sealed aluminum pan was used as reference, and the calibration of the DSC instrument was carried out using indium as standard. Thermogravimetric analysis (TGA) was performed with a Shimadzu TGA-51 thermal analyzer using platinum pans, flowing air at 50 mL min^{-1}, and a heating rate of 10°C min^{-1} from room temperature to 400°C.

Statistical analysis The reported data were obtained from mean values and the standard deviations are informed (mean ± SD). Statistical significance of the results was evaluated by one way ANOVA ($p < 0.05$) using the statistical tools available in the OriginPro v8.0 software.

RESULTS AND DISCUSSION

Effects of pH and temperature on PPO activity PPO from Hass avocado presents a maximum activity peak at pH 7.5 and a narrow plateau of lower activity at pH 4.5 (Fig. S1). Similar results were obtained with other varieties of avocado (13,30). Increasing the temperature from 10°C to 20°C enhances the enzymatic activity and the opposite effect is observed from 20°C to 45°C, the activity decreases at increasing temperature (Fig. S1). The maximum rate achieved at 20°C is consistent with the reported temperatures of other fruits PPOs like plums (31) and lower than the optimum temperatures of grapes and peaches PPOs (40°C) (26).

TABLE 1. Apparent formation constants (K_C) of paeonol and β-CD inclusion complex in aqueous solution at different temperatures.

Temperature (°C)	Slope	S_0 (mM)	Stoichiometry	K_C (M^{-1})	R^2
25	0.638	0.73	1:1	2388 ± 220	0.9899
30	0.541	0.78	1:1	1520 ± 194	0.9757
35	0.496	1.02	1:1	965 ± 87	0.9825
40	0.460	1.25	1:1	681 ± 46	0.9907
45	0.282	1.33	1:1	302 ± 13	0.9946

K_C value are reported as a mean value ± standard deviation (n = 3).

Thermal stability The thermal stability of the crude avocado PPO extract was tested from 20°C to 60 C° after 10, 20, 30 and 40 min of incubation and the results are reported in Table S1. The residual activity percentage ($A\%$) was calculated with the following equation:

$$A\% = \frac{A}{A_0} \times 100 \quad (1)$$

A and A_0 are the activities measured with and without thermal treatment, respectively. The enzyme was stable after incubation for 30 min at 20°C, then the residual activity percentage decreases to 72% after 40 min of incubation. The thermal stability profile indicates that long time exposures are required to achieve an efficient inactivation. Even at the most severe treatment (60°C for 40 min) PPO kept around 26% of its initial activity. The thermal inactivation process was analyzed with a first order kinetic model and the rates constants (k) (1/min) were calculated. The Arrhenius equation for the temperature dependence of k was used to estimate the activation energy (E_a). Using catechol as substrate, the E_a for the thermal inactivation of PPO was 64.54 kJ/mol, in agreement with the E_a reported for other PPOs (13,26).

Phase solubility diagrams of paeonol and β-CD The aim of this work is the evaluation of the inhibition properties of paeonol on the avocado PPO activity. Since this compound presents a very low aqueous solubility, the formation of an inclusion complex with β-CD was analyzed. Phase solubility diagrams of paeonol with β-CD were built following the Higuchi–Connors methodology (32). The solubility diagrams indicate a linear increase in the paeonol aqueous solubility with β-CD concentration in the range under study. This system can be classified as A_L-type, suggesting that the drugs solubility is enhanced through complexation with β-CD (Fig. S2). The apparent formation constants (K_C) and stoichiometric ratio of the inclusion complex can be determined from the linear phase solubility diagrams, using the following relationships:

$$S_t = \frac{m\, K_C S_0^m [\beta - CD]}{1 + K_C S_0^m} \quad (2)$$

In Eq. 2, S_t and S_0 are the total solubility and the intrinsic solubility of paeonol (without β-CD), respectively. When the S_t values are plotted against the [β-CD] and fitted with Eq. 2, the stoichiometry of the inclusion complex can be derived. Slopes values lower than 1 are indicative of 1:1 stoichiometry ($m = 1$) while slopes between 1 and 2 are obtained for 2:1 complexes ($m = 2$) (32). Additionally, the K_C values can be estimated from the slope and intercept of the linear fit. In Table 1, the formation constant of the paeonol inclusion complexes with β-CD measured in aqueous solutions at different temperatures are listed. The stoichiometry obtained from the slope of the linear regression analysis between 25°C and 45°C is 1:1. From the K_C values it is observed that the stability of the paeonol:β-CD complex increase at lower temperatures. The thermodynamic parameters of this inclusion process, enthalpy change ($\Delta H°$), entropy change ($\Delta S°$) and Gibbs energy change ($\Delta G°$) can be obtained by means of the classical van't Hoff equation:

$$\ln K_C = -\frac{\Delta H^\circ}{RT} + \frac{\Delta S^\circ}{R} \quad (3)$$

Eq. 3 is valid only if there is a linear variation of ln K_C with 1/T, or in other words, when $\Delta H°$ and $\Delta S°$ are independent on the temperature ($\Delta Cp \approx 0$) in the range considered. The thermodynamic parameters of the paeonol:β-CD inclusion complex where calculated with Eq. 3 and the following results were obtained: $\Delta H° = -77.64 \pm 7.37$ kJ/mol, $\Delta S° = -195.34 \pm 23$ J/K mol, and $\Delta G°_{298K} = -26.11 \pm 0.24$ kJ/mol.

The sign and magnitude of $\Delta H°$ and $\Delta S°$ can be related to the different driving forces of the inclusion process. It is known that hydrophobic effects, electrostatic and van der Waals interactions, hydrogen bonding and charge-transfer process are often involved in the formation of inclusion complexes with CDs (18,33). The hydrophobic effects are related to small and positive $\Delta H°$ and large and positive $\Delta S°$, making the inclusion process entropy driven while van der Waals interactions are related to negative $\Delta H°$ and $\Delta S°$. The thermodynamic parameters of the paeonol:β-CD complex indicate that the inclusion complex is enthalpy driven ($\Delta H° < 0$) with an unfavorable entropic term ($\Delta S° < 0$). Although different forces take place in the complex formation, the calculated $\Delta H°$ and $\Delta S°$ values suggests that the studied process is mainly governed by van der Waals interactions.

Solid state characterization of the inclusion complex The paeonol:β-CD inclusion complex was synthesized in solid state

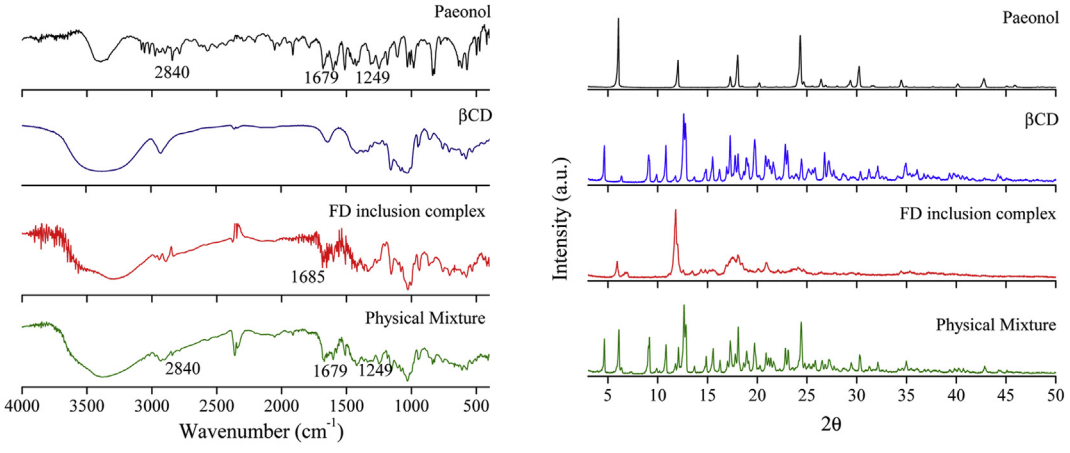

FIG. 1. FTIR spectra (left) and powder X-ray diffractograms (right) of paeonol, β-CD, the FD inclusion complex and the physical mixture.

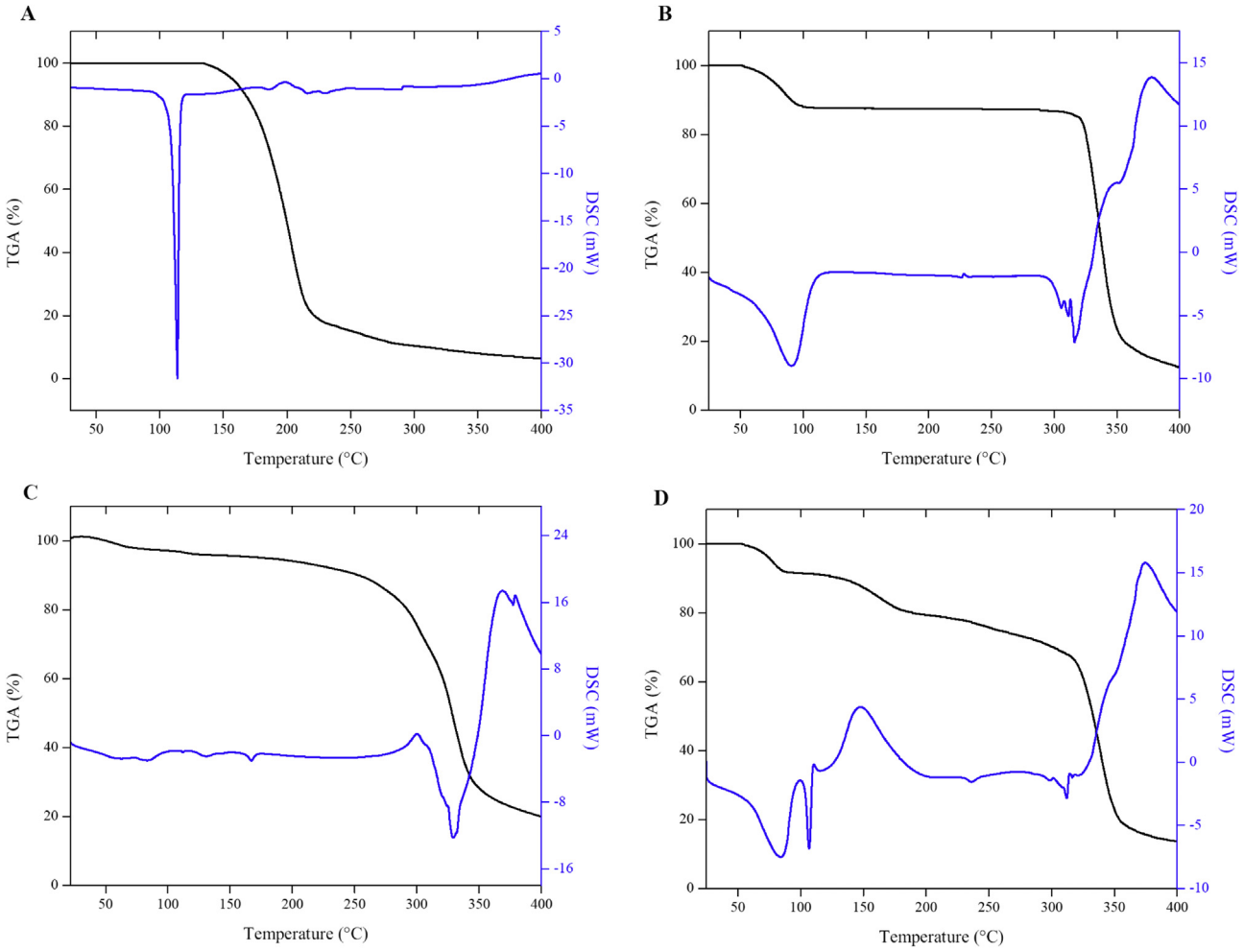

FIG. 2. DSC (blue lines) and TGA (black lines) curves of (A) free paeonol, (B) β-CD, (C) paeonol:β-CD FD inclusion complex and (D) the physical mixture.

using a freeze-dried method (FD). This sample was further characterized with FTIR spectroscopy and PXR diffractometry. In Fig. 1, the FTIR spectra of paeonol, β-CD, the FD inclusion complex and the physical mixture are depicted. Paeonol presents the characteristic signal at 1679 cm^{-1} assigned to the carbonyl stretching band (υC=O). The symmetric and antisymmetric C–H stretchings of the methoxyl group are found at 2840 and 2899 cm^{-1}, and the O–CH_3 stretching is located at 1249 cm^{-1}. A band is also observed at 3880 cm^{-1}, assigned to the stretching of the OH group (34). The formation of the inclusion complex with β-CD in the FD sample induces a small shift on the paeonol υC=O band to 1685 cm^{-1}, suggesting a reinforcement in the bond strength. Similar shifts were observed in the inclusion complexes with other carbonyl compounds. A possible explanation to this observation is that the intramolecular H-bond of the free drug is weakened upon complexation with β-CD (18,35), increasing the strength of the C=O bond. Another change in the complex spectrum is the slight shift towards higher wavenumber of the υO-CH_3 band located at 1249 cm^{-1}, overlapping with other paeonol bands. This shift is not observed in the PM sample, suggesting an interaction of this group with the β-CD inner cavity in the FD complex. This idea is supported by the disappearance of the υC-H band from the O–CH_3 group located at 2840 cm^{-1} in the complex spectrum. All these changes are indicative that the inclusion complex formation takes place in the solid state and suggest that the interactions between β-CD and paeonol involve the C=O, OH and O–CH_3 groups of the later. These changes are not observed in the PM sample.

X-ray diffractometry has been widely used in the characterization of CDs and their inclusion complexes in powder or microcrystalline state. The appearance in the inclusion complex sample of new diffraction peaks, as well as the shift of characteristic peaks of the guest molecule, together with changes in their relative intensity, are all indicative of the formation of a new solid phase (36). Fig. 1 shows the PXR diffractograms of the solid samples. Paeonol presents sharp diffractions peaks at 6.0, 12.0, 18.0 and 24.4 and the diffraction pattern of β-CD also indicates the crystalline nature of this compound. The diffractogram of the PM sample is a direct superposition of the signals present in the individual patterns of paeonol and β-CD, suggesting that the inclusion complex is not formed by simply mixing the solid reactants. However, the diffraction pattern of the FD sample is very different from the corresponding patterns of paeonol and β-CD. Some peaks of paeonol (6.0 and 12.0) are still present in the FD diffractogram but their relative intensities are changed and a small shift from 12.0 to 11.62 is observed. In addition, the peak at 24.4 disappears with an important loss of crystallinity observed between 15.0 and 30.0°, suggesting that a new phase is obtained in this sample. Characteristics peaks of β-CD 4.6, 9.13, 10.84 and 12.64 observed in the PM are not present in the FD binary mixture. These changes can be taken as an evidence for the formation of true inclusion complex between paeonol and β-CD in solid state.

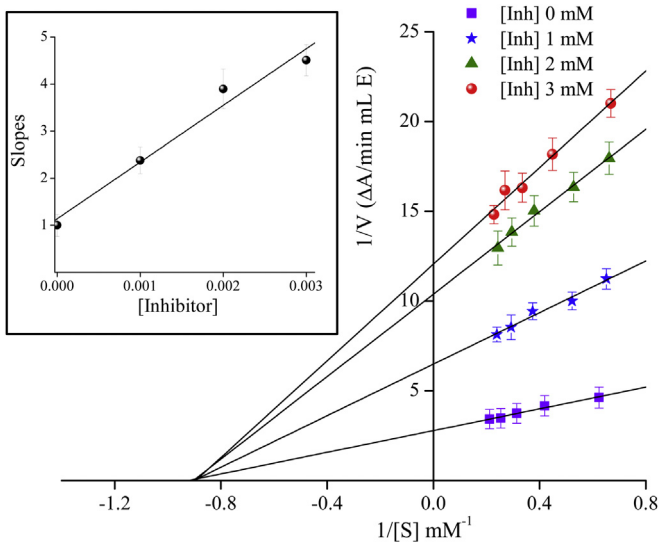

FIG. 3. Inhibition of avocado PPO by paeonol at different concentrations of the inhibitor using catechol as substrate. Error bars indicate the standard deviation of each data point (n = 3). Inset: graphical determination of the inhibitor constant K_i.

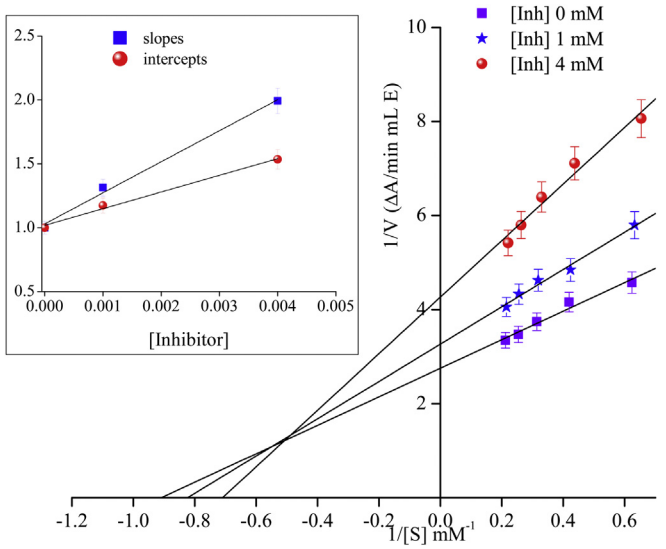

FIG. 4. Inhibition of avocado PPO by β-CD at different concentrations of the inhibitor using catechol as substrate. Error bars indicate the standard deviation of each data point (n = 3). Inset: graphical determination of the inhibitor constants K_i and $K_{i'}$.

Thermal analysis of the paeonol:β-CD inclusion complex In order to complete the solid state characterization, a thermal analysis was performed. The DSC and TGA curves of the paeonol, β-CD, FD and PM samples are illustrated in Fig. 2. Paeonol shows a sharp endothermic peak at 107.67°C, corresponding to the melting process (Fig. 2A), while the TGA curve exhibits a major weight loss (94.33%) between 177.23°C and 218.21°C, corresponding to the decomposition of the drug. The DSC analysis of β-CD shows a broad endothermal event at 93.95°C associated with a mass loss of 11.76% in the TGA curve (Fig. 2B) corresponding to their dehydration. This weight loss is related to the loss of eight water molecules from the β-CD cavity (18). The events observed between 288°C and 335°C with a mass loss of 74.86% are related to the decomposition of this compound. Fig. 2C represents DSC and TGA curves of the FD sample. The disappearance of the melting peak of paeonol and the reduction of the β-CD dehydration signal are evidence the complex formation. In addition, the dehydration with a weight loss of 3.17% (two water molecules) is found at lower temperature, between 52.71°C and 69.82°C. The inclusion of paeonol reduced the number and the bond strength of the water molecules included in the β-CD cavity. Moreover, the FD inclusion complex exhibits the decomposition events of paeonol at higher temperatures, between 308.47°C and 343.48°C. These results suggest that the inclusion complex increase the thermal stability of paeonol. The DSC curve of the PM sample (Fig. 2D) presents the endothermal events corresponding to the melting process of paeonol, the dehydration of β-CD, and the decomposition of each compound.

***In vitro* inhibition of avocado PPO** The inhibitory effects of paeonol and β-CD, separately, on the avocado PPO activity were examined using catechol as substrate. In addition, 4-hydroxy-benzaldehyde, a typical PPO inhibitor (26,37), was also tested for comparison purposes. Paeonol and 4-hydroxy-benzaldehyde solutions were prepared in ethanol (for solubility reasons) and β-CD in water. The kinetic data were analyzed with Linewaver-Burk plots and good correlations were obtained from the linear regressions. Different concentrations of each inhibitor were employed in order to elucidate the inhibition mechanism and the results are presented in Figs. 3 and 4 and Table 2. Increasing concentrations of paeonol reduce V_{max} of the browning process but the K_M values are not affected. This behavior is characteristic of a non-competitive inhibition mechanism. 4-hydroxy-benzaldehyde presents the same type of inhibition than paeonol (Fig. S3). Moreover, from the slopes of the Lineweaver–Burk plots, the apparent inhibition constants K_i were calculated (Fig. 3, inset). The calculated K_i values are 0.831 mM for paeonol and 0.913 mM for 4-hydroxy-benzaldehyde. On the other hand, β-CD reduces the V_{max} and increases the K_M values of the reaction, although higher concentrations are required to achieve the same degree of inhibition than the other inhibitors tested. From Fig. 4, a mixed-type inhibition can be proposed for β-CD. The same inhibition mechanism has been proposed for β-CD using PPO extracted form apples and potatoes (38,39). In this case, $K_{i'}$ (7.68 mM) > K_i (4.12 mM), meaning that β-CD bind to the free enzyme and to the enzyme-substrate complex as well, with a higher affinity for the free PPO (39). These *in vitro* results showed that paeonol can be considered as a good inhibitor of avocados PPO, having a similar efficiency than 4-hydroxy-benzaldehyde (a well-known PPO inhibitor). However, the use of this compound as a food additive is considerably limited because of its poor aqueous solubility, since organic solvents, such as ethanol, are necessary for appropriate drug dissolution. For this reason, the paeonol:β-CD complex was also tested as PPO inhibitor. Aqueous

TABLE 2. Kinetic parameters (V_{max} and K_M) for the inhibition of avocado PPO using different inhibitors concentrations (mM).

Inhibitor	V_{max} (UE·ml^{-1})	K_M (mM)	$V_{max}/K_M \cdot 10^{-3}$ (UE·ml^{-1}·mM^{-1})
Without inhibition	3594 ± 125	1.085 ± 0.091	3.31
4-Hydroxybenzaldehyde			
1	2261 ± 71	1.166 ± 0.118	1.94
2	1349 ± 32	1.160 ± 0.085	1.16
3	801 ± 23	1.143 ± 0.098	0.70
Paeonol			
1	1542 ± 63	1.107 ± 0.096	1.39
2	941 ± 25	1.162 ± 0.060	0.81
3	821 ± 29	1.117 ± 0.086	0.74
β-CD			
1	3060 ± 101	1.231 ± 0.085	2.52
4	2340 ± 123	1.409 ± 0.125	1.66
Paeonol:β-CD			
1	1111 ± 55	0.992 ± 0.102	1.12

Results are reported as a mean value ± standard deviation (n = 3).

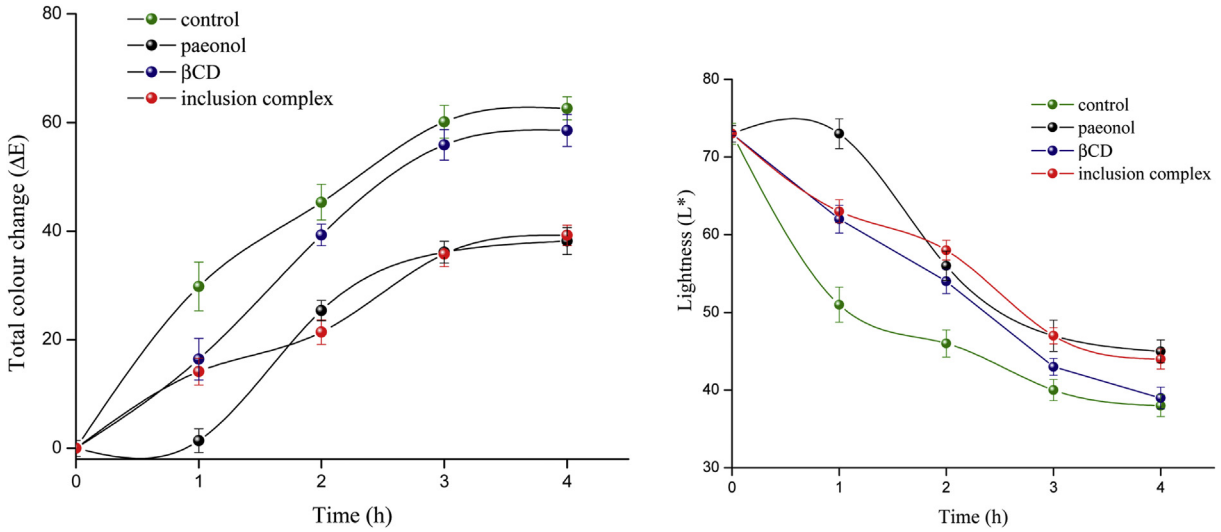

FIG. 5. Effect of different inhibitors on the evolution of total color change (ΔE) (left) and lightness (L^*) (right) in fresh avocado pulp. Error bars indicate the standard deviation of each data point (n = 3).

solutions of the inclusion complex were prepared with a concentration of 1 mM and the inhibition efficiency was compared with free paeonol and β-CD. The Lineweaver–Burk plot for the enzymatic inhibition of the inclusion complex is depicted in Fig. S4 and the V_{max} and K_M values are listed in Table 2. From this table it is observed that an ethanolic solution of paeonol (1 mM) induces a 57% reduction of V_{max} (37% for 4-hydroxy-benzaldehyde) while an aqueous solution of the inclusion complex (also 1 mM) reduces the reaction V_{max} by 70%. It can be concluded that the formation of the paeonol:β-CD inclusion complex not only enhances the aqueous solubility of the guest drug, but also enhances the inhibition efficiency against avocado PPO.

***In vivo* inhibition of avocado PPO** The *in vitro* results obtained it the section above are very useful for understanding the inhibition capacity and mechanism of a given compound. However, these studies are performed under controlled conditions (pH, temperature, exogenous substrate at fixed concentrations), which may vary significantly from the conditions observed in the fresh vegetables. Moreover, some compounds exhibit strong inhibition capacity from *in vitro* experiments but this effect is reduced (or disappear) when is measured from *in vivo* experiments (40). For this reason, the inhibitory effects of paeonol and the inclusion complex were tested directly on the avocado fresh pulp. The browning reaction was followed measuring the total color change (ΔE^*), a single parameter calculated from the L^* a^* b^* values according to the following equation:

$$\Delta E^* = \left[\left(\Delta L^*\right)^2 + \left(\Delta a^*\right)^2 + \left(\Delta b^*\right)^2\right]^{1/2} \quad (4)$$

This parameter, together with L^* are frequently employed to evaluate color changes in fruits and vegetables pulps (41). The measurements made at time 0 were used for the calculation of the Δ values of each parameter. In Tables S2–S5, the L^* a^* b^* and ΔE^* values are listed for the color evolution of the fresh avocado pulp treated with 1 mM solution of paeonol, β-CD and the inclusion complex for a time period of 4 h. It can be observed that the browning produces changes in the color of the avocado pulp, evolving from green to red and decreasing the blue composition towards yellow tones. This is deduced by the changes towards less negative values of a^* and b^*. In addition, the inhibitors have little effect in the changes towards red or in the loss of green tones (a^* parameter). However, paeonol and its inclusion complex retard changes towards yellows, since their variation of b^* are smaller. In Fig. 5, the lightness (L^*) and color changes (ΔE^*) of the samples are shown. It is observed that after 1 h paeonol is the best inhibitor, because it is able to keep the L^* value that the avocado sample had in the initial time. β-CD and the inclusion complex have a comparable efficiency; although a decrease in the initial lightness is produce, the decrease in this parameter is lower than in the control sample. After 3 h, the three inhibitors show similar results, and the overlap produced in the behavior of paeonol and its inclusion complex is particularly highlighted, indicating the efficiency of the complexation to solubilize paeonol and preserve its inhibitory action. After 4 h, these two inhibitors continue to have similar effects on the lightness of the samples, and in turn have a higher inhibitory activity to that of β-CD (the L^* value with this inhibitor is almost the same than the control). At this final time, it is important to note that both paeonol and its inclusion complex preserve the lightness value of the avocado, achieving similar results to those that would be obtained at 2 h in the control sample.

As a summary, a kinetic analysis reveals a non-competitive mechanism for the inhibition of avocado PPO by paeonol and a mixed-type mechanism for β-CD. Solubility diagrams show that the formation of the 1:1 paeonol:β-CD inclusion complex improves the aqueous solubility of paeonol. The formation of the complex in solid state was also confirmed by FTIR spectroscopy and powder X-ray diffraction. This solid formulation also improves the thermal stability of the drug. In addition the paeonol:β-CD inclusion complex improves the *in vitro* inhibition of PPO compared with free paeonol and free β-CD. The *in vivo* results present some differences with respect to those *in vitro*, suggesting that the inclusion complex does not increase the inhibitory effect of paeonol, but in any case allows it to be used in aqueous solutions. As the browning reaction proceeds on the avocado pulp, a decrease in lightness and total color changes is observed in all samples. However, changes in both parameters were less pronounced in the samples containing paeonol or its inclusion complex. The important biological properties associated with paeonol, together with the results obtained in this work, make the paeonol:β-CD inclusion complex a possible candidate to the formulation of food additives, aimed to prevent or decrease the enzymatic browning. Although these results were obtained with avocado PPO, paeonol and its complex are likely to have similar effects on other PPOs, so their application could be extended to other fields of food industry.

Supplementary data to this article can be found online at https://doi.org/10.1016/j.jbiosc.2018.11.009.

ACKNOWLEDGMENTS

This work was supported by Secretaria de Ciencia y Tecnica of Universidad Nacional de San Luis [grant number 2-2118]; and the Agencia Nacional de Promoción Científica y Tecnológica [grant number 2015-1003 FONCyT] from Argentina.

References

1. **Friedman, M.:** Food browning and its prevention: an overview, J. Agric. Food Chem., **44**, 631–653 (1996).
2. **Burton, S.:** Biocatalysis with polyphenol oxidase: a review, Catal. Today, **22**, 459–487 (1994).
3. **Muñoz-Pina, S., Ros-Lis, J., Arguelles, A., Coll, C., Martínez-Mañez, R., and Andres, A.:** Full inhibition of enzymatic browning in the presence of thiol-functionalised silica nanomaterial, Food Chem., **241**, 199–205 (2018).
4. **Sikora, M. and Swieca, M.:** Effect of ascorbic acid postharvest treatment on enzymatic browning, phenolics and antioxidant capacity of stored mung bean sprouts, Food Chem., **239**, 1160–1166 (2018).
5. **Mohsenabadi, M., Ghasemnezhad, M., Hashempour, A., and Hasan Sajedi, R.:** Inhibition of polyphenol oxidases and peroxidase activities in green table olives by some anti-browning agents, Agric. Conspec. Sci., **82**, 375–381 (2017).
6. **Chutintrasri, B. and Noomhorm, A.:** Thermal inactivation of polyphenoloxidase in pineapple puree, LWT Food Sci. Technol., **39**, 492–495 (2006).
7. **Lante, A., Tinello, F., and Nicoletto, M.:** UV-A light treatment for controlling enzymatic browning of fresh-cut fruits, Innov. Food Sci. Emerg. Technol., **34**, 141–147 (2016).
8. **Cao, X., Cai, C., Wang, Y., and Zheng, X.:** The inactivation kinetics of polyphenol oxidase and peroxidase in bayberry juice during thermal and ultrasound treatments, Innov. Food Sci. Emerg. Technol., **45**, 169–178 (2018).
9. **Noci, F., Riener, J., Walkling-Ribeiro, M., Cronin, D., Morgan, D., and Lyng, J.:** Ultraviolet irradiation and pulsed electric felds (pef) in a hurdle strategy for the preservation of fresh apple juice, J. Food Eng., **85**, 141–146 (2008).
10. **Zhou, L., Liu, W., Xiong, Z., Zou, L., Chen, J., Liu, J., and Zhong, J.:** Different modes of inhibition for organic acids on polyphenoloxidase, Food Chem., **199**, 439–446 (2016).
11. **Hu, Y.-H., Liu, X., Jia, Y.-L., Guo, Y.-J., Wang, Q., and Chen, Q.-X.:** Inhibitory kinetics of chlorocinnamic acids on mushroom tyrosinase, J. Biosci. Bioeng., **117**, 142–146 (2014).
12. **Xiong, Z., Liu, W., Zhou, L., Zou, L., and Chen, J.:** Mushroom (agaricus bisporus) polyphenoloxidase inhibited by apigenin: multi-spectroscopic analyses and computational docking simulation, Food Chem., **203**, 430–439 (2016).
13. **Weemaes, C., Ludikhuyze, L., Van Den Broeck, I., Hendrickx, M., and Tobback, P.:** Activity, electrophoretic characteristics and heat inactivation of polyphenoloxidases from apples, avocados, grapes, pears and plums, LWT Food Sci. Technol., **31**, 44–49 (1998).
14. **Toledo, L. and Aguirre, C.:** Enzymatic browning in avocado (*persea americana*) revisited: history, advances, and future perspectives, Crit. Rev. Food Sci. Nutr., **57**, 3860–3872 (2017).
15. **Ha, D., Trung, T., Hien, T., Dao, T., Yim, N., Ngoc, T., Oh, W., and Bae, K.:** Selected compounds derived from Moutan Cortex stimulated glucose uptake and glycogen synthesis via AMPK activation in human hepG2 cells, J. Ethnopharmacol., **131**, 417–424 (2010).
16. **Hsieh, C.-L., Cheng, C.-Y., Tsai, T.-H., Lin, I.-h., Liu, C.-H., Chiang, S.-Y., Lin, J.-G., Lao, C.-J., and Tang, N.-Y.:** Paeonol reduced cerebral infarction involving the superoxide anion and microglia activation in ischemia-reperfusion injured rats, J. Ethnopharmacol., **106**, 208–215 (2006).
17. **Sun, G.-P., Wang, H., Xu, S.-P., Shen, Y.-X., Wu, Q., Chen, Z.-D., and Wei, W.:** Anti-tumor effects of paeonol in a HepA-hepatoma bearing mouse model via induction of tumor cell apoptosis and stimulation of IL-2 and tnf-α production, Eur. J. Pharmacol., **584**, 246–252 (2008).
18. **Sancho, M. I., Russo, M. G., Moreno, M. S., Gasull, E. I., Blanco, S. E., and Narda, G. E.:** Physicochemical characterization of 2-hydroxybenzophenone with β-cyclodextrin in solution and solid state, J. Phys. Chem. B, **119**, 5918–5925 (2015).
19. **Rakmai, J., Cheirsilp, B., Mejuto, J. C., Simal-Gandara, J., and Torrado-Agrasar, A.:** Antioxidant and antimicrobial properties of encapsulated guava leaf oil in hydroxypropyl-beta-cyclodextrin, Ind. Crop. Prod., **111**, 219–226 (2018).
20. **Astray, G., Gonzalez-Barreiro, C., Mejuto, J. C., Rial-Otero, R., and Simal-Gandara, J.:** A review on the use of cyclodextrins in foods, Food Hydrocolloids, **23**, 1631–1640 (2009).
21. **Yildiz, A., Celebioglu, Z. I., Kilic, M., Durgun, E., and Uyar, T.:** Menthol/cyclodextrin inclusion complex nanofibers: enhanced water-solubility and high-temperature stability of menthol, J. Food Eng., **224**, 27–36 (2018).
22. **Cravotto, G., Binello, A., Baranelli, E., Carraro, P., and Trotta, F.:** Cyclodextrins as food additives and in food processing, Curr. Nutr. Food Sci., **2**, 343–350 (2006).
23. **Rakmai, J., Cheirsilp, B., Mejuto, J. C., Torrado-Agrasar, A., and Simal-Gandara, J.:** Physico-chemical characterization and evaluation of bio-efficacies of black pepper essential oil encapsulated in hydroxypropyl-betacyclodextrin, Food Hydrocolloids, **65**, 157–164 (2017).
24. **Zhu, T.-H., Yu, Y.-Y., and Cao, S.-W.:** Tyrosinase inhibitory effects and antioxidant properties of paeonol and its analogues, Food Sci. Technol. Res., **19**, 609–615 (2013).
25. **Tsai, Y., Tsai, H.-H., Wu, C.-P., and Tsai, F.-J.:** Preparation, characterisation and activity of the inclusion complex of paeonol with β-cyclodextrin, Food Chem., **120**, 837–841 (2010).
26. **Garro, A. and Gasull, E.:** Characterization of polyphenoloxidase from 2 peach (*Prunus persica L.*) varieties grown in Argentina, Food Sci. Biotechnol., **19**, 627–632 (2010).
27. **Rocha, A., Cano, M., Galeazzi, M., and Morais, A.:** Characterisation of 'starking' apple polyphenoloxidase, J. Sci. Food Agric., **77**, 527–534 (1998).
28. **Lineweaver, H. and Burk, D.:** The determination of enzyme dissociation constants, J. Am. Chem. Soc., **56**, 658–666 (1934).
29. **Quevedo, R., Jaramillo, M., Diaz, O., Pedreschi, F., and Aguilera, J.:** Quantification of enzymatic browning in apple slices applying the fractal texture Fourier image, J. Food Eng., **95**, 285–290 (2009).
30. **Gomez-Lopez, V.:** Some biochemical properties of polyphenol oxidase from two varieties of avocado, Food Chem., **77**, 163–169 (2002).
31. **Siddiq, M., Sinha, N., and Cash, J.:** Characterization of polyphenoloxidase from stanley plums, J. Food Sci., **57**, 1177–1179 (1992).
32. **Connors, K.:** Measurement of cyclodextrin complex stability constants, pp. 205–242, in: Szejtli, J. and Osa, T. (Eds.), Comprehensive supramolecular chemistry, vol. 3: Cyclodextrins. Elsevier (1996).
33. **Brewster, M. and Loftsson, T.:** Cyclodextrins as pharmaceutical solubilizers, Adv. Drug Deliv. Rev., **59**, 645–666 (2007).
34. **Arjunan, V., Devi, L., Subbalakshmi, R., Rani, T., and Mohan, S.:** Synthesis, vibrational, NMR, quantum chemical and structure-activity relation studies of 2-hydroxy-4-methoxyacetophenone, Spectrochim. Acta A, **130**, 164–177 (2014).
35. **Sancho, M., Andujar, S., Porasso, R., and Enriz, R.:** Theoretical and experimental study of inclusion complexes of β-cyclodextrins with chalcone and 2,4-dihydroxychalcone, J. Phys. Chem. B, **120**, 3000–3011 (2016).
36. **Mura, P.:** Analytical techniques for characterization of cyclodextrin complexes in aqueous solution: a review, J. Pharmaceut. Biomed. Anal., **101**, 238–250 (2014).
37. **Yi, W., Cao, R., Peng, W., Wen, H., Yan, Q., Zhou, B., Ma, L., and Song, H.:** Synthesis and biological evaluation of novel 4-hydroxybenzaldehyde derivatives as tyrosinase inhibitors, Eur. J. Med. Chem., **45**, 639–646 (2010).
38. **Singh, V., Jadhav, S., and Singhal, R.:** Interaction of polyphenol oxidase of solanum tuberosum with β-cyclodextrin: process details and applications, Int. J. Biol. Macromol., **80**, 469–474 (2015).
39. **Alvarez-Parrilla, E., de la Rosa, L., Rodrigo-Garcia, J., Escobedo-Gonzalez, R., Mercado-Mercado, G., Moyers-Montoya, E., Vazquez-Flores, A., and Gonzalez-Aguilar, G.:** Dual effect of β-cyclodextrin (β-CD) on the inhibition of apple polyphenol oxidase by 4-hexylresorcinol (hr) and methyl jasmonate (mj), Food Chem., **101**, 1346–1356 (2007).
40. **Nerya, O., Ben-Arie, R., Luzzatto, T., Musa, R., Khativ, S., and Vaya, J.:** Prevention of agaricus bisporus postharvest browning with tyrosinase inhibitors, Postharvest Biol. Technol., **39**, 272–277 (2006).
41. **Falguera, V., Sanchez-Riaño, A., Quintero-Ceron, J., Rivera-Barrero, C., Mendez-Arteaga, J., and Ibarz, A.:** Characterization of polyphenol oxidase activity in juices from 12 underutilized tropical fruits with high agroindustrial potential, Food Bioprocess Technol., **5**, 2921–2927 (2012).